New Modulated Molecular Beam Scattering Methods for Probing Nonlinear and Coverage-Dependent Reaction Kinetics at Surfaces

D. F. Padowitz,† K. A. Peterlinz, and S. J. Sibener*

The James Franck Institute and The Department of Chemistry, The University of Chicago, Chicago, Illinois 60637

Received April 10, 1991. In Final Form: July 29, 1991

A new *three* molecular beam arrangement is introduced that expands the range and power of modulated beam reactive scattering for studying complex kinetics at surfaces. This paper presents two types of kinetic measurements that utilize this three-beam arrangement. The first measurements use two continuous, independently adjustable molecular beams to establish steady-state reaction conditions, while a weaker modulated third beam induces small concentration perturbations around the selected steady state. This technique permits experimental linearization of nonlinear kinetics over a wide range of conditions, allowing us to explore the global behavior of reactions, determine coverage-dependent rate constants, and isolate individual elementary steps from complex reaction mechanisms. We illustrate these capabilities with preliminary results for the oxidation of hydrogen to water and for the recombination kinetics of hydrogen on the Rh(111) surface. The second group of measurements uses time-resolved specular helium scattering as a sensitive in situ probe of both adsorbate coverage and coverage-dependent surface kinetics. The oxidation of CO on Rh(111) under pseudo-first-order conditions is examined with this new kinetic probe.

I. Introduction

Molecular beam scattering techniques have firmly established themselves among the major tools for studying the kinetics and dynamics of gas–surface interactions. Modulated molecular beam relaxation spectrometry (MBRS), a descendent of Eigen's pioneering work on chemical relaxation,[1] extracts kinetic information by analyzing product evolution in response to a time-varying reactant beam flux. Relaxation techniques based on this principle are now widely used in reactive scattering to study heterogeneous chemical reactions.

The evaluation of surface kinetic data by transform analysis of modulated beam measurements was introduced in an early paper by Foxon, Boudry, and Joyce and has since been well studied.[2] Transform analysis, widely used in electrical engineering and linear systems theory, determines the properties of a system by its response to a known input. Fourier or Laplace transforms are used to deconvolute a "transfer function", characteristic of the system, from the observed output to a given periodic or transient input. Transform analysis of MBRS data is straightforward when the product response to changing reactant flux is linear.[3] Accordingly, most studies reported to date have been on simple linear reactions, such as single-component adsorption–desorption at low coverage, have used linear approximations for weakly nonlinear systems, or have worked in a pseudo-first-order regime over a limited coverage range.[4-8]

In this paper we introduce several particularly useful extensions to conventional MBRS techniques, which expand the range of reaction types and reaction conditions that can be studied with molecular beam techniques. Our ultimate goal is to study heterogeneous reactions, in the linearized limit, under arbitrarily chosen and precisely defined reactant coverage regimes. Our measurements are all based on the experimental strategy of performing kinetic measurements by observing the relaxation from small density perturbations, which we have experimentally introduced around carefully defined steady-state reaction conditions.

Most chemical systems are not linear. An elementary bimolecular step in a chemical reaction involves two species and the rate of reaction depends on the product of their concentrations. If both concentrations change with time, the rate expression for the mechanism will be nonlinear. A reaction will also be nonlinear if the rate constants change with concentration. This is frequently true for surface reactions, in which adsorption probabilities, preexponential factors, and activation energies often depend on coverages.

Besides prohibiting experimental deconvolution and the use of Fourier transform analysis methods that depend on linear response, nonlinearity frequently presents other severe mathematical difficulties in analyzing chemical reaction mechanisms. A model reaction mechanism yields a set of ordinary differential equations describing the experimentally observable rates. For nonlinear differential equations there are no general mathematical techniques providing analytical solutions. Numerical integration of nonlinear differential equations may be difficult since rate constants for elementary reaction steps may range over many orders of magnitude, leading to a set of "stiff" differential equations, creating numerical instabilities.

However, it is often possible experimentally to constrain the reaction to a linear regime. If this is done, linear transform analysis may be applied to the experimental data, and the differential equations for a postulated mechanism may be solved by series expansions or perturbation techniques, allowing the sought after kinetic information to be obtained. The pioneers in the field, including Foxon, Olander, Madix, Weinberg, and their co-workers,[2-8] were aware of the problems of nonlinear kinetics and examined linearized MBRS, but the theory outstripped the available

† Current address: Department of Chemistry, University of California, Berkeley, CA 94720.

(1) Eigen, M. In *Technique of Organic Chemistry*; Interscience: New York, 1963; Vol. VIII, Part II, p 901.
(2) Foxon, C. T.; Boudry, M. R.; Joyce, B. A. *Surf. Sci.* **1974**, *44*, 69.
(3) Chang, H.-C.; Weinberg, W. H. *J. Chem. Phys.* **1977**, *66*, 4176.
(4) Olander, D. R.; Ullman, A. *Int. J. Chem. Kinet.* **1976**, *8*, 625.
(5) Schwarz, J. A.; Madix, R. J. *Surf. Sci.* **1974**, *46*, 317.
(6) Jones, R. H.; Olander, D. R.; Siekhaus, W. J.; Schwarz, J. A. *J. Vac. Sci. Technol.* **1972**, *9*, 1429.
(7) Sawin, H. H.; Merrill, R. P. *J. Vac. Sci. Technol.* **1981**, *19*, 40.
(8) D'Evelyn, M. P.; Madix, R. J. *Surf. Sci. Rep.* **1984**, *3*, 413.

0743-7463/91/2407-2566$02.50/0

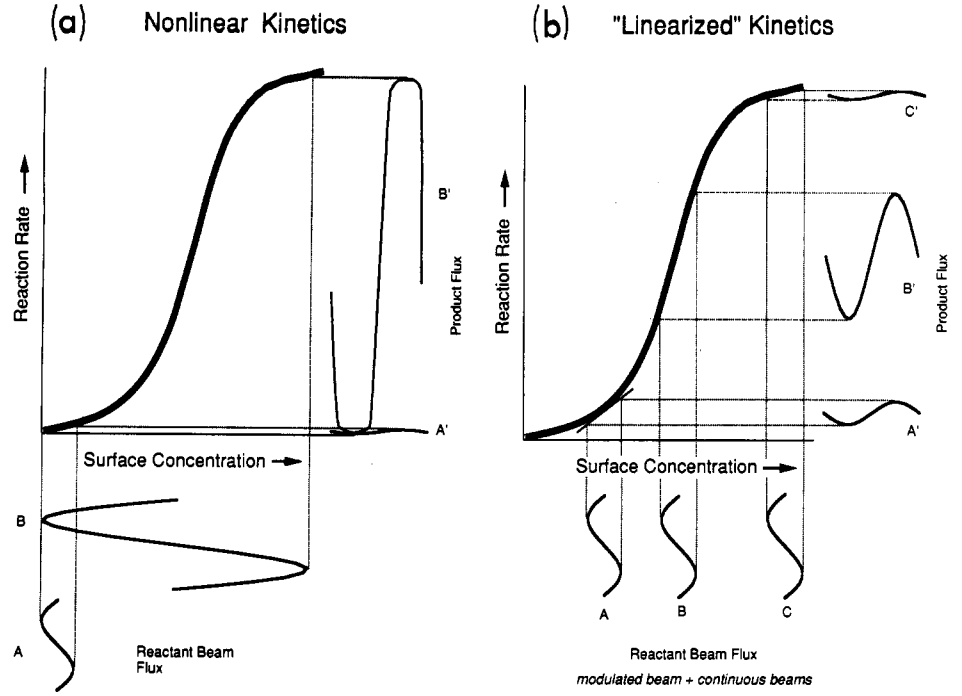

Figure 1. Different modulation schemes that can be used during surface-reactive scattering experiments. Part a is of the conventional type, with reactant density spanning a large range of coverage during the modulation cycle. Part b, after Foxon et al.,[2] which utilizes small perturbations of reactant density during each modulation cycle, portrays a scheme that is now possible with our new three-beam approach.

instrumentation. In succeeding years the numerous successes of MBRS obscured its limitations, which have only recently been reconsidered as more complex situations are encountered.[9]

Let us now consider the general problem of conducting modulated beam experiments on nonlinear systems and discuss a general solution to the problem. Figure 1a presents a schematized view of a conventional experimental arrangement. When a small modulated beam flux is used (scheme A, Figure 1a), the response may be linear but is restricted to a low-coverage regime. Depending on the shape of the order plot, there may be little signal at all. When an intense modulated beam is used (scheme B, Figure 1a), a wide coverage range is spanned during each modulation cycle, producing a nonlinear response that is difficult to analyze. This "strong modulation" scheme can further complicate matters by inducing time-dependent behavior in other reactants and reaction intermediates. Stated simply, one of the main consequences of this typical method is that the measured kinetics represent a convolution over all coverages on the surface.

Ideally, one would like to avoid these problems by sampling the kinetics under isosteric conditions. The straightforward solution is to establish a steady-state reaction on the surface with arbitrarily chosen adsorbate coverages and to then superimpose a small modulation about the selected steady state. Such a scenario is shown in Figure 1b. Modulation schemes A–C here, i.e., for three different coverages, all involve sufficiently small excursions from the preset steady state that relaxation is linear. If this linearization could be performed experimentally for different steady-state conditions, then reaction mechanisms or coverage dependencies of the rate constants may be determined over the global range of conditions for the nonlinear reaction.

This paper introduces a new *three* molecular beam scattering arrangement, which allows us to directly implement the approach described above and provides greater versatility for new methods. The scheme is depicted in Figure 2. We use two continuous, independently adjustable beams to establish a selected steady state on the surface, while a weaker modulated third beam induces small concentration perturbations around the selected steady state. This is not the only way to linearize an MBRS experiment, but it is simple and direct, retains the advantages of molecular beam sources, and offers great flexibility in experimental design. In addition to linearization by means of weak modulation, we can use the continuous beams to move away from the near-zero coverage limit in which molecular beam experiments are sometimes forced to work, and to widely vary steady-state surface coverages, which is important for determining coverage-dependent activation energies and preexponential factors. Most significantly, by controlling reactant and intermediate coverage regimes, sometimes using isotopic substitutions in the beams, we can isolate the individual elementary steps that compose complex reaction mechanisms.

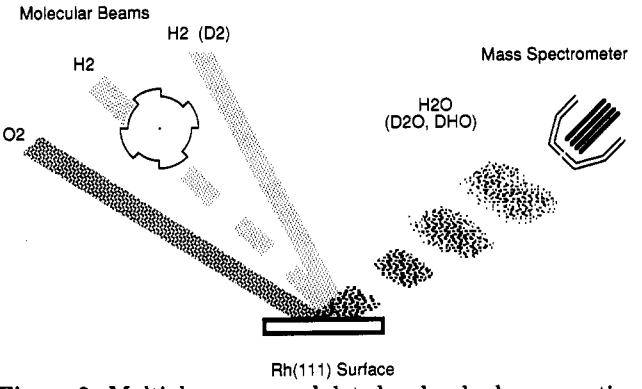

Figure 2. Multiple-source modulated molecular beam reactive scattering. Two continuous beam sources establish steady-state surface conditions, which are perturbed by a third modulated beam in order to probe kinetics.

(9) Engstrom, J. R.; Weinberg, W. H. *J. Chem. Phys.* **1987**, *87*, 4211.

This experimental approach is not without difficulties. The two most significant complications are extreme sensitivity requirements and the need for in situ coverage assessment. Signal levels will be smaller than those encountered in conventional MBRS measurements since the modulation depth (i.e., the surface coverage change induced by the incident modulated molecular beam) has to be reduced in order to reach the linearized limit. This limit has now been reached for the simple $H_2 + D_2 \rightarrow HD$ and the more complicated $H_2 + D_2 + O_2 \rightarrow HDO$ reactions, as will be discussed later in this paper. These two problems have now been addressed in our group by using time-resolved helium specular scattering to assess adsorbate coverage, to determine the modulation depth, and to directly measure reaction kinetics. The basis for this technique is the extraordinarily large scattering cross section that adsorbates have for reducing specular helium reflectivity. The origin of this effect has been well documented[10-12] and is due to the long-range attractive part of the adsorbate–helium interaction potential. In this paper we shall demonstrate for the CO oxidation reaction that helium reflectivity measurements conducted during modulated beam reactive scattering measurements can be used as a kinetic response "*amplifier*", gaining back much of the signal that was lost by using much smaller modulation depths than are commonly used in conventional MBRS measurements.

II. Experimental Section

For this work, a third beam source was installed in the UHV surface scattering instrument used in our previous studies of CO oxidation on Rh(111).[13,14] The apparatus consists of a removable source chamber containing three supersonic molecular beam sources and a main chamber with sample and manipulator, mass spectrometer detector, residual gas analyzer, Auger spectrometer, and sputter ion gun.

The source chamber is divided laterally into two sections, each with three differential regions of diffusion pumping before the main chamber. The left beam is in one section and the center and right beams together are in the other. The supersonic expansion in each beam originated from ≈100-μm pinholes and was formed by a skimmer, collimator, and shutter. The center beam was modulated by a rotating chopper wheel with a four-slot 50% total duty cycle pattern, or a dual pattern chopper with two 25% slots and two 1% slits for incident beam time-of-flight measurements.

On entering the main chamber, the left and right beams were defined by 80-mil apertures and the center beam was defined by a 40-mil aperture. The beams passed through a final differential pumping region before the scattering region. The main chamber scattering region was pumped primarily by a 400 L/s ion pump. The base pressure in the scattering region was 5×10^{-11} Torr, rising to 6×10^{-9} Torr at the highest beam fluxes.

The distance from chopper to sample was 21.21 cm. The left and right beams were 15° off axis. The sample normal was usually at 45° to the beam axis, resulting in roughly 5 × 7 mm elliptical spots on the sample, which overlapped the center 2.5 × 3.25 mm modulated beam spot. Maximum side beam flues were on the order of 10 langmuir/s, or 10^{-5} Torr/cm^2.

A rhodium single-crystal sample was cut and polished by standard techniques. The surface was within $^1/_2$° of the FCC (111) plane, as determined by Laue X-ray diffraction. The surface was prepared in UHV by cycles of Ar ion sputtering and heating in oxygen and was kept very clean by oxidation and reduction during the experimental reaction. Surface cleanliness was verified with Auger spectroscopy and, subsequently, with specular helium reflectivity measurements.

The detector is an Extranuclear quadrupole mass spectrometer, doubly differential pumped by two 50 L/s ion pumps and an additional Balzers 50 L/s turbomolecular pump on the ionizer region. Transmitted ions are detected with a Venetion blind electron multiplier, suitable for pulse counting. Angular acceptance of the detector is 1°. Flight path from sample to ionizer is 14.45 cm. At normal, the detector views a spot of ≈2.5-mm diameter.

Product time of arrival wave forms were acquired by a custom multichannel scalar system triggered by the photodetector on the chopper wheel assembly, collecting 255 channels of 5–20 μs. For the water reaction, good quality wave forms usually required 10–60 min of signal averaging. A typical run of 20 min at 400 Hz chopper speed would be 5×10^5 chopper periods or "shots", giving 5×10^4 counts/channel with signal to background of 2, and S/N of 200.

III. Results

A. Three-Beam Scattering and Mechanism Linearization. We being this section by examining the oxidation of hydrogen to form water on the Rh(111) surface. This reaction is relatively complicated and has attracted considerable attention.[15]

There are several sources of nonlinearity in this mechanism. Hydrogen sticking probabilities and desorption rate parameters depend on both hydrogen and oxygen coverages.[16,17] As the reaction probably proceeds by sequential H + O and H + OH addition or OH disproportionation, the differential equations for the overall mechanism contain several terms that are quadratic in hydrogen coverage. These quadratic terms prohibit general solutions of the rate equations for this mechanism.

Experimentally, an examination of the rate of water production for different hydrogen and oxygen beam intensities (Figure 3) shows that no global "order" can be assigned to the reactants. The data for this coverage-dependent order map were obtained with three beams. Continuous H_2 and O_2 beam pressures were varied to establish the desired steady-state reaction. The third molecular beam, which in this instance was H_2, was modulated at 100 Hz for phase-sensitive detection. The rate of product formation rapidly saturates as hydrogen flux is increased for all oxygen fluxes measured. For high hydrogen beam intensities, the reaction is linear in oxygen coverage, but at low hydrogen flux, the yield is nonmonotonic, first increasing, then decreasing again as oxygen flux increases.

Time domain measurements for water production further emphasize the nonlinear nature of MBRS wave forms taken with arbitrarily chosen modulation strengths. With three beam sources, we are able to combine a modulated H_2 beam with continuous beams of D_2 and O_2 to produce three isotopically substituted forms of water. This arrangement was shown in Figure 2. Figure 4 shows mass spectrometer signal vs time wave forms for the three products of this reaction. The H_2O wave form has the usual symmetric form. The HDO product, however, shows a highly asymmetric wave form, with a rapid rise, sloping top, and long decay. As will be shown below, this appearance is the same as that for HD produced in an

(10) Poelsema, B.; Comsa, G. *Scattering of Thermal Energy Atoms from Disordered Surfaces*; Springer Tracts in Modern Physics 115; Springer-Verlag: Berlin, 1989.
(11) Poelsema, B.; Palmer, R. L.; Comsa, G. *Surf. Sci.* **1984**, *136*, 1.
(12) Poelsema, B.; Comsa, G. *Faraday Discuss. Chem. Soc.* **1985**, *80*, 247.
(13) Brown, L. S.; Sibener, S. J. *J. Chem. Phys.* **1988**, *89*, 1163.
(14) Brown, L. S.; Sibener, S. J. *J. Chem. Phys.* **1989**, *90*, 2807.
(15) Norton, P. R. In *The Chemical Physics of Solid Surfaces and Heterogeneous Catalysis*; King, D. A., Woodruff, D. P., Eds.; *Fundamental Studies of Heterogeneous Catalysis*; Elsevier: New York, 1982; Vol. 4.
(16) Thiel, P. A.; Yates, J. T., Jr.; Weinberg, W. H. *Surf. Sci.* **1979**, *90*, 121.
(17) Yates, J. T., Jr.; Thiel, P. A.; Weinberg, W. H. *Surf. Sci.* **1979**, *84*, 427.

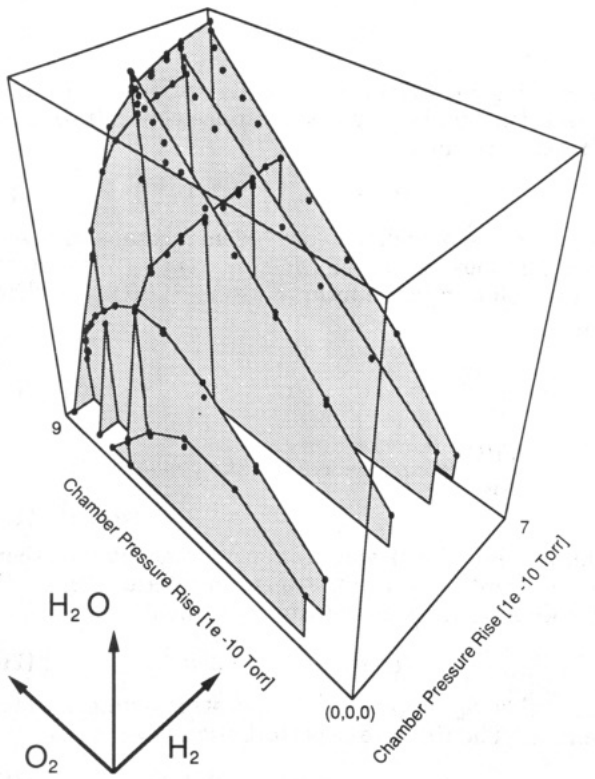

Figure 3. Steady-state water production vs reactant beam flux. The pressure rise in the chamber calibrates the hydrogen and oxygen beam fluxes. No global "order" can be assigned to the reactants based on the relationship of reactant flux to H_2O production.

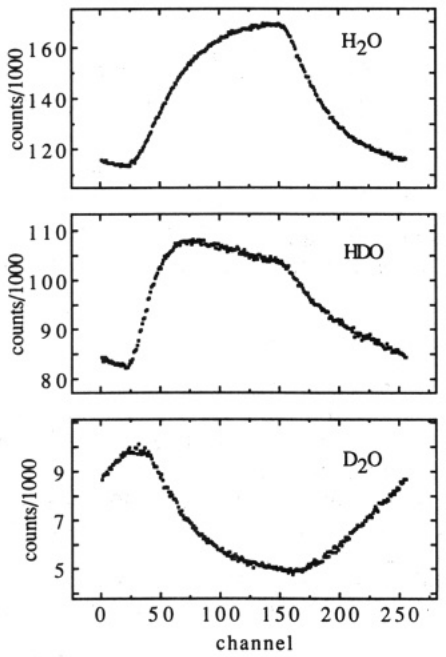

Figure 4. Mass spectrometer time-of-arrival wave forms of the products from modulated H_2 and continuous D_2 and O_2 beams reacting on Rh(111) at 665 K. The channel time is 10 μs/channel. The ratio of modulated to continuous beams is high. The HDO response is nonlinear and the D_2O background shows negative modulation. Note that neither D_2 nor O_2 beam is modulated and that the D_2O modulation is solely due to perturbation of the steady-state surface coverages of O, D, and OD by the modulated H_2 beam.

overdriven modulation cycle. This nonlinearity is due to the changing coverage of D species on the surface during the H_2 pulse. The most remarkable wave form is that for D_2O, which shows *negative* modulation. Remember that

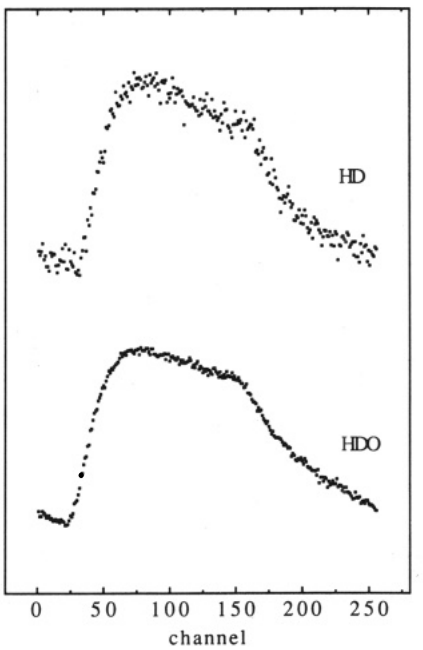

Figure 5. HDO and HD wave forms. The essential features of the asymmetric HDO wave form are also seen in an HD wave form, indicating that the origin of the nonlinearity is similar in both reactions.

neither D_2 nor O_2 was modulated in this experiment. On first glance one would expect a continuous background signal of D_2O to be produced from this arrangement. The negative modulation gives a direct measure of the extent to which the modulated H_2 beam perturbs the steady-state coverages of O, D, and OD.

The origin of the nonlinearity and the mathematical analysis can be best illustrated in the simpler HD recombination reaction. Figure 5 shows that the HD and HDO wave forms share the same asymmetric shape. This can be quantitatively understood by examining the reaction mechanism and by then numerically simulating the result. The mechanism for this reaction can be modeled as

$$H_{2gas} \underset{k_d}{\overset{s_0(1-([H]+[D]))}{\rightleftarrows}} 2H \quad (1)$$

$$D_{2gas} \underset{k_d}{\overset{s_0(1-([H]+[D]))}{\rightleftarrows}} 2D \quad (2)$$

$$H + D \xrightarrow{K_d} HD_{gas} \quad (3)$$

This mechanism can be simulated by numerical integration of the system:

$$\frac{d[H]}{dt} = 2P_{H_2}(1 - ([H] + [D])) - 2k_d[H]^2 - k_d[H][D] \quad (4)$$

$$\frac{d[D]}{dt} = 2P_{D_2}(1 - ([H] + [D])) - 2k_d[D]^2 - k_d[H][D] \quad (5)$$

$$d[HD]_{gas}/dt = k_d[H][D] \quad (6)$$

where P incorporates the incident beam flux and the zero-coverage sticking coefficient.

The qualitative behavior does not depend on the rate constants, only on the ratio of the continuous and modulated fluxes. Figure 6 shows the simulated results, and corresponding Fourier transfer function plots (showing the product phase and amplitude for all input frequencies), for three different ratios of the modulated D_2 intensity to

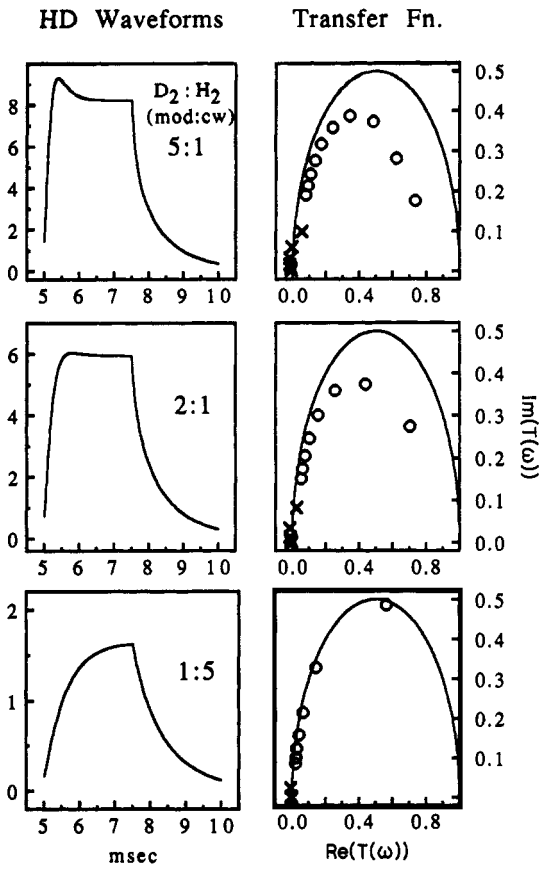

Figure 6. HD simulation vs modulation strength. As the strong modulation is reduced, the wave form becomes more symmetric, the odd harmonics of the transfer function approach the single-step arc, and the even harmonics vanish—all indications that the kinetics are approaching a linear regime.

the continuous H_2 intensity. The 5:1 (strong modulation limit) plot shown in Figure 6 resembles the HD wave form of Figure 5. Examinationa of the simulation shows that the rapid rise is due to the increase in adsorbed H, the sagging top to decline in adsorbed D. The long tail is the recovery of D as H decreases; the product of the two drops less quickly than H alone. The transfer function, shown to the right, does not fall on the "semicircle" as a single-step reaction would.[5,6] More importantly, significant even harmonics appear. Since the reactant beam modulated by the chopper is a square wave, it contains only odd harmonics, and the presence of even frequencies in the response indicates nonlinearity. In the strong modulation limit, as the modulated D coverage increases the steady-state D coverage drops—the overall kinetics are therefore nonlinear as the kinetic equations depend on the product of two time-varying quantities. Reducing the relative intensity of the modulated beam reduces the nonlinearity, as seen in the second and third panels of Figure 6. Here, we clearly see that as the modulation is decreased, the wave form becomes symmetric, the transfer function approaches the single-step arc, and the even harmonics vanish. In this weak perturbation limit the reaction becomes linear.

Finally, we perform a perturbation theory analysis of the data to extract the desired kinetic information from the linearized wave forms. Note that a perturbation treatment allows us to analytically solve the differential equations for the HD mechanism, yielding physical insight into the elementary steps of the reaction. The reaction is second order in hydrogen concentration, and thus nonlinear:

$$H_{2gas} \underset{k}{\overset{s}{\rightleftharpoons}} 2H \tag{7}$$

The sticking coefficient is s, the desorption rate k. Let the reactant flux be P and the surface concentration of hydrogen [H], then

$$d[H]/dt = 2sP - 2k[H]^2 \tag{8}$$

Now consider a small time-dependent flux superimposed on a continuous background $P = p_0 + \epsilon p(t)$. We wish to obtain a solution in the form $[H] = h_0 + \epsilon h(t)$. We then have

$$\frac{d(h_0 + \epsilon h(t))}{dt} = 2s(p_0 + \epsilon p(t)) - 2k(h_0 + \epsilon h(t))^2 \tag{9}$$

$$\frac{d(h_0)}{dt} + \epsilon \frac{dh(t)}{dt} = 2sp_0 + \epsilon 2sp(t) - 2kh_0^2 - 4k\epsilon h_0 h(t) - 2k\epsilon^2 h(t)^2 \tag{10}$$

If this is to hold for all values of ϵ over some interval, then the coefficients of each power of ϵ must equate. For zeroth order we have the steady-state component

$$dh_0/dt = 0 = 2sp_0 - 2kh_0^2 \tag{11}$$

This yields $h_0 = (sp_0/k)^{1/2}$, the steady-state surface coverage. The first-order perturbation is

$$dh(t)/dt = 2sp(t) - 4kh_0 h(t) \tag{12}$$

This is the desired linear response. Substituting the steady-state h_0

$$dh(t)/dt = 2sp(t) - 4kh(t)\sqrt{sp_0/k} \tag{13}$$

or

$$dh(t)/dt = 2sp(t) - k'h(t) \tag{14}$$

where the effective rate constant $k' = 4(skp_0)^{1/2}$. In Arrhenius form we have

$$A' \exp(-E'/kT) = 4\sqrt{sp_0 A \exp(-E/kT)} \tag{15}$$

with $A' = 4(sp_0A)^{1/2}$ and $E' = E/2$. Finally, we relate the measured rates for the linearized system to the actual rates:

$$A = A'^2/16sp_0 \qquad E = 2E' \tag{16}$$

The activation energy is obtained directly, the preexponential requires knowledge of the beam flux and sticking coefficient, or of the steady-state coverage h_0. A similar analysis may be found in ref 5.

An Arrhenius plot of our experimental pseudo-first-order rates is shown in Figure 7. The pseudo-first-order rate constants are $E'_a = 10.0$ kcal/mol, $A' = 10^7$ s^{-1}. The true second-order constants are $E_a = 20$ kcal/mol, $A = 10^{-2}$ cm^{-2}/s. This is in good agreement with earlier work.[17-19]

We now return to the water reaction and demonstrate that the linearized limit can also be reached for this more complicated system (before the signal becomes too small to detect!). Figure 8 is a plot of the even harmonics in the Fourier transform of the HDO product wave form.[7] Since the reactant beam modulated by the chopper is a square wave, it contains only odd harmonics, and the presence of even frequencies in the response indicates nonlinearity. As the strength of the modulation is reduced, the per-

(18) Engle, T.; Kuipers, H. *Surf. Sci.* **1979**, *90*, 162.
(19) Verheij, L. K.; Hugenschmidt, M. B.; Anton, A. B.; Polesma, B.; Comsa, G. *Surf. Sci.* **1989**, *210*, 1.

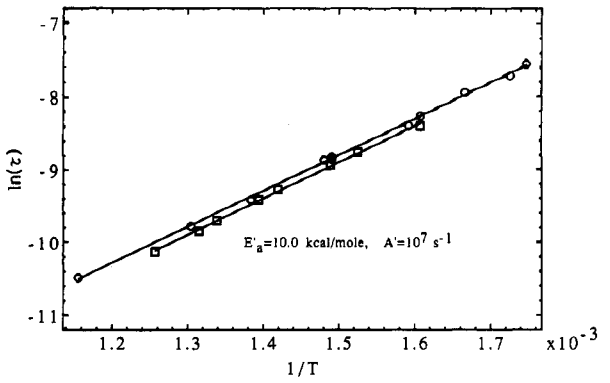

Figure 7. HD Arrhenius plot. The linearized or pseudo-first-order rates for H + D recombination are plotted for two runs differing slightly in continuous beam flux. The true second-order rates are derived from them as described in the text: $E_a = 2E'_a$; the preexponential is approximately 10^{-2} cm²/s, using an estimated continuous beam flux of 10 ML/s.

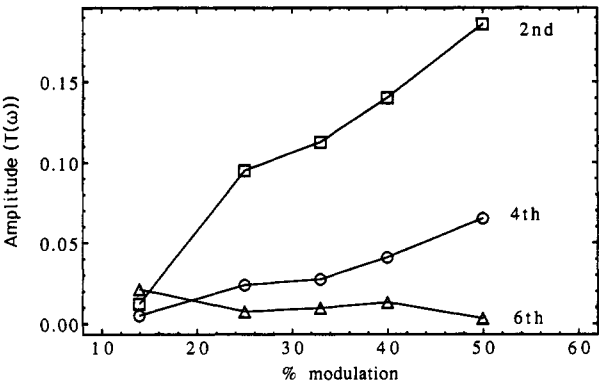

Figure 8. Linearization of the HDO response. The amplitude of the even harmonics of the HDO wave form indicates nonlinearity. Modulation is measured as the ratio of the modulated beam to the sum of modulated H_2 and continuous D_2 beams. With smaller modulation, the amplitudes of the even harmonics systematically decrease and approach zero as the response becomes linear.

turbation measured by the depression of D_2O production decreases and the amplitudes of the even harmonics decrease. Modulation is measured as the ratio of the modulated beam to the sum of modulated H_2 and continuous D_2 beams. The perturbation of steady-state surface coverage can be determined from the transient depression of the continuous D_2O background. The perturbation decreases from 60% to less than 5% as the intensity of the modulation is reduced. With smaller perturbations, the response becomes more linear. The even harmonics approach zero, clearly demonstrating the experimental linearization of the kinetics in the limit of weak modulations. More extensive results for hydrogen oxidation[20] and $H_2 + D_2$ recombination[21] on Rh(111) are forthcoming.

B. Helium Reflectivity as an in Situ Probe of Surface Coverage and Kinetics. As shown above, the use of three beam sources provides excellent control of reactant flux, but an in situ method of assessing adsorbate surface concentration is also necessary in order to extract the desired kinetic rate constants. Furthermore, signal levels in the linearized limit can be extremely low since much smaller modulation depths are used than in conventional single-beam MBRS experiments. These two problems have now been addressed in our group by using

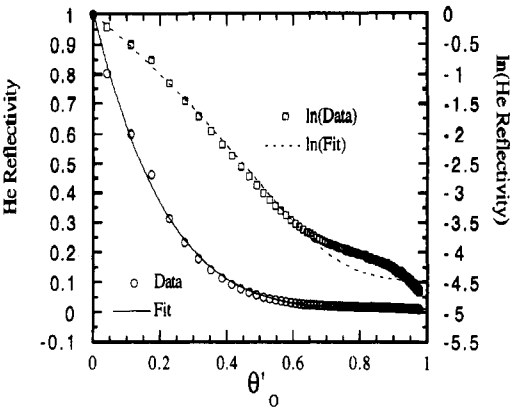

Figure 9. Specular helium reflectivity vs relative oxygen coverage. Solid and dashed lines are the calculated fits to the data using eq 17. Parameters obtained from the fit to the data: $\Sigma_O = 44.2$ Å² and $B = 0.826$. Experimental conditions: $T_S = 525$ K, $E_i = 63$ meV, and $\theta_i = \theta_f = 45°$.

time-resolved helium specular scattering to assess adsorbate coverage, reactant modulation depth, and even reaction kinetics when warranted. In this section we shall demonstrate for the CO oxidation reaction that helium reflectivity measurements conducted during modulated beam reactive scattering measurements can be used as a kinetic response "*amplifier*", gaining back much of the signal that was lost by using much smaller modulation depths than are commonly used in conventional MBRS measurements.

This extremely sensitive method for making in situ coverage and kinetic measurements of surface reactions utilizes specular He scattering to directly monitor adsorbate coverages. Poelsema and Comsa[10-12] demonstrated that the large He scattering cross sections from disordered adsorbates on low index surfaces results in a sharp attenuation of the specular He signal as adsorbate coverages increase. A relatively simple model accounts for the attentuation by assuming that the cross section for diffusely scattering the He wave can be associated with the (large) elastic scattering cross section that exists between the He atom and the adsorbate. Allowing for a random overlap, they derived a "lattice gas formula":

$$I_{\theta_A}/I_{00} = (1 - \theta_A)^{\Sigma_A \eta} \qquad (17)$$

I_{00} is the specular He intensity from the bare surface, I_{θ_A} is the specular He intensity at coverage θ of species A, Σ_A is the cross section associated with that molecule for the selected incident angle and beam energy, and η is the surface atom density. The ratio I_{θ_A}/I_{00} is defined here as the He reflectivity for that adsorbate coverage. As shown in Figure 9, He reflectivity was calibrated against surface coverage by utilizing thermal desorption or, in this case, titration to determine relative coverages. Here we dosed a Rh(111) surface with O_2 and monitored the He reflectivity for a room-temperature, i.e., 63-meV, He beam at 45° incident angle and then we determined the relative oxygen coverages at various dosing times by titrating the adsorbed oxygen with CO and measuring the resultant CO_2 signal. We can then plot He reflectivity against the relative O coverage, θ'_O, where 1 represents a saturated disordered O overlayer. Disordering, measured by the disappearance of diffraction peaks, occurs below 400 K with no new ordering at higher temperatures. Since the absolute O coverage (relative to the Rh atom density), θ_O, was unknown, we fit our data to eq 1 with $\theta_O = B\theta'_O$ where θ'_O is the measured coverage, and B is the absolute O coverage relative to the Rh atom density. Equation 17 fits our data up to $\theta'_O = 0.65$, with $\Sigma_O = 44.2$ Å², $\eta = 0.13$

(20) Padowitz, D. F.; Sibener, S. J. *Surf. Sci.* **1991**, *254*, 125.
(21) Padowitz, D. F.; Sibener, S. J. *J. Vac. Sci. Technol. A* **1991**, *9*, 2289.

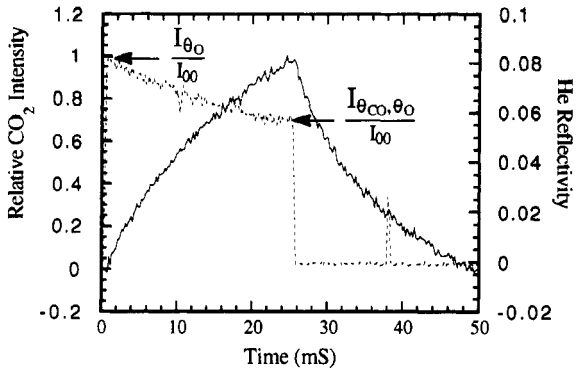

Figure 10. CO_2 intensity and He reflectivity wave forms for CO oxidation on 525 K Rh(111). The CO_2 wave form, the solid line, was Fourier analyzed to give a rate constant, while the He wave form was analyzed to give reactant coverages during the reaction. The combination of information derived from the two wave forms allowed us to determine the coverage-dependent reaction rate constant. For this case with T_S = 525 K and at the He reflectivity derived oxygen coverage of 0.350, we find K' = 55 s^{-1}.

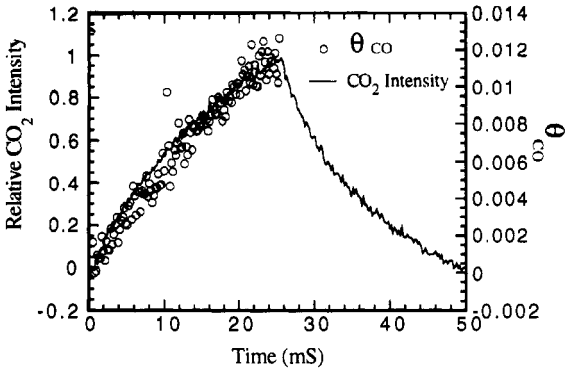

Figure 11. CO_2 intensity and θ_{CO} wave forms for CO oxidation on Rh(111). θ_{CO} was calculated from the in situ He reflectivity. For the experimental conditions used, we find that the CO coverage varied from 0 to 1.2% during this scattering experiment. This 1.2% change is much less than the 35% oxygen coverage, clearly supporting the the assumption of pseudo-first-order kinetics. As seen in this figure, desorption rate constants obtained from the CO_2 wave form and the time-resolved He reflectivity data are, within experimental uncertainty, identical.

$Å^{-2}$, and B = 0.826. Root et al.[22] measured B = 0.83 using XPS. A similar experiment for CO on Rh(111) produced Σ_{CO} = 148 $Å^2$.[23]

The empirical calibrations, combined with the model calculations, were used to determine the in situ, instantaneous coverages of adsorbates in modulated molecular beam experiments. Here we present the example of CO oxidation reaction on Rh(111). Brown and Sibener[13] determined the reaction kinetics for CO oxidation in the low CO coverage regime by using a continuous O_2 beam and a modulated CO beam. The rate expression for this reaction is

$$d\theta_{CO}/dt = S_{CO}(\theta_O,\theta_{CO},T)I_{CO} - K(\theta_O,\theta_{CO},T)\theta_O\theta_{CO} \quad (18)$$

$$I_{CO_2} = K(\theta_O,\theta_{CO},T)\theta_O\theta_{CO} \quad (19)$$

I_{CO_2} is the time-dependent flux of CO_2 leaving the surface; θ_{CO} and θ_O are the time-dependent CO and O coverages, respectively; $S_{CO}(\theta_O,\theta_{CO},T)$ is the coverage and temperature-dependent sticking coefficient for CO; I_{CO} is the incident CO flux; and $K(\theta_O,\theta_{CO},T)$ is the coverage and temperature-dependent rate constant. For a sufficiently low CO intensity, θ_O is constant and the kinetics follow a pseudo-first-order behavior:

$$d\theta_{CO}/dt = S_{CO}(\theta_O,T)I_{CO} - K'(\theta_O,T)\theta_{CO} \quad (20)$$

$$I_{CO_2} = K'(\theta_O,T)\theta_{CO} \quad (21)$$

where $K'(\theta_O,T) = K(\theta_O,\theta_{CO},T)\theta_O$. K', the measured first-order rate constant, was determined from the phase lag of the first Fourier component of the product CO_2 wave form (solid line) in Figure 10.

In order to determine the steady-state oxygen coverage as well as the coverage-dependent sticking probability, a CO–He mixture is used for the incident modulated beam. I_O is determined for this beam by extrapolating from high-temperature (>650 K) measurements where CO has an insignificant residence time and thus no effect on the scattering intensity. During the modulated beam experiment, the rotatable mass spectrometer was changed to look at either the product CO_2 intensity at normal or the He intensity at specular. He reflectivity (dashed line) is calculated by dividing the experimental He scattering intensities by the extrapolated intensities determined immediately prior to immediately after the modulated beam kinetics measurements. Here a dual chopper wheel, with a square wave and time-of-flight pattern, is used to modulate the mixed CO–He beam. The He signal shown in Figure 10 therefore disappears at the midpoint of the CO_2 wave since the chopper blocks the incident beam.

Since both CO and O are adsorbed on the surface during the modulated beam experiment, there are two surface species to attenuate the He signal. The contribution from O was determined from the reflectivity at low θ_{CO} or low I_{CO_2}, where there is an insignificant contribution from adsorbed CO and thus the He reflectivity is largest. Here I_{θ_O}/I_{00} = 0.0825, which corresponds to θ_O = 0.350. The exponential decay in He signal after 0.5 ms is due to the rise if θ_{CO} during the open chopper part of the modulation period. Solving explicitly for this part of the wave form

$$\theta_{CO}(t) = \frac{S(\theta_O)I_{CO}}{K'(\theta_O,T)}(1 - \exp(K(\theta_O,T)t)) \quad (22)$$

I_{CO} can be measured from the direct beam flux, and K', the pseudo-first-order rate constant, can also be determined, as explained above. If $\theta_{CO}(t)$ can be determined from He reflectivity, as will be shown, and I_{CO} is known, then $S_{CO}(\theta_O)$ is readily calculable from eq 22.

Assuming that CO occupies random surface sites unoccupied by O and thus the area associated with the CO cross section overlaps randomly with O covered sites in the mixed overlayer, the cross section for small CO coverages can be expressed

$$I_{\theta_{CO},\theta_O}/I_{\theta_O} = \exp(-\eta\Sigma_{CO}\theta_{CO}/(1 - \theta_O)) \quad (23)$$

or

$$\theta_{CO} = -((1 - \theta_O)/\eta\Sigma_{CO}) \ln (I_{\theta_{CO},\theta_O}/I_{\theta_O}) \quad (24)$$

where I_{θ_O} is the He signal from the O-covered surface and $I_{\theta_O,\theta_{CO}}$ is the He signal from the CO- and O-covered surface. Figure 11 shows the comparison of the CO_2 desorption wave form to the θ_{CO} wave form calculated from the He wave form. The rate constant calculated from the θ_{CO} wave form is identical, within experimental error, with the rate constant from the CO_2 wave form, thus demonstrating the validity of this new method. So the coverage-dependent rate constants can be determined from the product wave forms and in situ He reflectivity measurements, or simply from the He scattering measurements by themselves, since the measurements monitor the time

(22) Root, T. W.; Schmidt, L. D.; Fisher, G. B. *Surf. Sci.* **1983**, *134*, 30.

evolution of the surface species. With the addition of flux meters to our machine to measure the incident reactant flux, we can use the He reflectivity derived reactant coverage to determine the coverage-dependent sticking coefficients as well. By combining product wave form measurements with in situ He reflectivity measurements, we can measure and characterize the coverage-dependent behavior of the kinetic parameters, the rate constants, coverages, and sticking coefficients for a wide range of incident reactant pressures and surface temperatures. This approach is general and will work well for any surface chemical system that has at most two well-characterized adsorbates on a low index surface.

IV. Conclusion

In this paper we have described several particularly useful extensions to conventional MBRS techniques, which expand the range of reaction times and reaction conditions that can be studied with molecular beam techniques. The methods discussed employ independently adjustable, continuous sources of each reactant to establish steady-state conditions on the surface, which are then perturbed by a modulated flux of one reactant. In situ specular helium scattering from the same modulated beam can then be used to assess or confirm coverages, modulation depths, sticking coefficients, and reaction rates.[23] This approach allows us to explore nonlinear reaction kinetics using a very general combination of experimental and analytical strategies based on linearity in the limit of small perturbations around a steady state.

(23) Peterlinz, K. A.; Curtiss, T. J.; Sibener, S. J. *J. Chem. Phys.*, in press.

This limit has now been reached for the simple $H_2 + D_2 \rightarrow HD$ and the more complicated $H_2 + D_2 + O_2 \rightarrow HDO$ reactions, adding to the success of the $CO + O_2 \rightarrow CO_2$ system. When linearized, the coupled differential equations that described reaction kinetics can be solved by perturbation theory, yielding physical insight into reaction mechanisms for *arbitrarily chosen* and *precisely measured* surface coverage regimes. Both HD and HDO reactions have been moved from nonlinear to linear regimes by reducing the intensity of the modulated flux relative to continuous reactant flux, and the reactant coverages used in the CO_2 reaction have been calibrated and measured precisely with in situ He scattering.

To date we have been concerned with controlling surface reactant coverages in order to examine reaction rates. At a more fundamental level, chemisorption energies have been observed to change with coverage.[16] In the future our focus will move from kinetics to dynamics, by probing the disposal of reaction exoergicity into product degrees of freedom as a function of coverage. This will allow us to examine in greater detail how adsorbate density changes the potential energy surfaces that govern heterogeneous reactions.

Acknowledgment. This work was supported in part by the Office of Naval Research and by the NSF Materials Research Laboratory program at the University of Chicago (NSF-DMR-8819860).

Registry No. H_2, 1333-74-0; H, 12385-13-6; CO, 630-08-0; Rh, 7440-16-6.